

CADET: Context-Conditioned Ads CTR Prediction With a Decoder-Only Transformer

David Pardoe*

Neil Daftary*

Miro Furtado*

Aditya Aiyer*

LinkedIn

Mountain View, California, USA

dpardoe@linkedin.com

Yu Wang

Liuqing Li

Tao Song

Lars Hertel

LinkedIn

Mountain View, California, USA

ywang11@linkedin.com

Young Jin Yun

Senthil Radhakrishnan

Zhiwei Wang†

Tommy Li

LinkedIn

Mountain View, California, USA

yyun@linkedin.com

Khai Tran

Ananth Nagarajan

Ali Naqvi

Yue Zhang

LinkedIn

Mountain View, California, USA

khtran@linkedin.com

Renpeng Fang

Avi Romascanu

Arjun Kulothungun

Deepak Kumar

LinkedIn

Mountain View, California, USA

refang@linkedin.com

Praneeth Boda

Fedor Borisyuk

Ruoyan Wang*

LinkedIn

Mountain View, California, USA

rnwang@linkedin.com

Abstract

Click-through rate (CTR) prediction is fundamental to online advertising systems. While Deep Learning Recommendation Models (DLRMs) with explicit feature interactions have long dominated this domain, recent advances in generative recommenders have shown promising results in content recommendation. However, adapting these transformer-based architectures to ads CTR prediction still presents unique challenges, including handling post-scoring contextual signals, maintaining offline-online consistency, and scaling to industrial workloads.

We present CADET (Context-Conditioned Ads Decoder-Only Transformer), an end-to-end decoder-only transformer for ads CTR prediction deployed at LinkedIn. Our approach introduces several key innovations: (1) a context-conditioned decoding architecture with multi-tower prediction heads that explicitly model post-scoring signals such as ad position, resolving the chicken-and-egg problem between predicted CTR and ranking; (2) a self-gated attention mechanism that stabilizes training by adaptively regulating information flow at both representation and interaction levels; (3) a timestamp-based variant of Rotary Position Embedding (RoPE) that captures temporal relationships across timescales from seconds to months; (4) session masking strategies that prevent the model from learning dependencies on unavailable in-session events, addressing train-serve skew; and (5) production engineering techniques including tensor packing, sequence chunking, and custom Flash Attention kernels that enable efficient training and serving at scale.

In online A/B testing, CADET achieves a 11.04% CTR lift compared to the production LiRank [3] baseline model, a hybrid ensemble of DCNv2 [18] and sequential encoders. The system has been successfully deployed on LinkedIn’s advertising platform, serving the main traffic for homefeed sponsored updates.

CCS Concepts

- **Information systems** → **Computational advertising**; Online advertising;
- **Computing methodologies** → **Neural networks**; *Deep learning*.

Keywords

Click-Through Rate Prediction, Generative Recommenders, Online Advertising

1 Introduction

LinkedIn is the world’s largest professional social network, serving over one billion members globally, with a leading B2B-focused advertising platform. Homefeed sponsored updates represent the primary surface for LinkedIn ads, where click-through rate (CTR) prediction serves as the core model powering ad delivery and determining which ads are displayed to users. The accuracy and efficiency of CTR prediction therefore directly impacts both LinkedIn user experience and advertiser outcomes.

Historically, Deep Learning Recommendation Model (DLRM) architectures [17, 24], which focus on explicit feature interaction learning, have dominated ads CTR prediction. These models typically operate on individual ad impressions with a large number of engineered features. More recently, generative recommenders based on decoder-only transformers have demonstrated success in industrial applications [8, 10, 22], primarily in feed content recommendation and e-commerce domains. These models process user interaction sequences autoregressively, learning implicit temporal patterns.

However, adapting decoder-only transformers to production-grade ads CTR prediction still presents unique challenges. First, post-scoring contextual signals such as ad position significantly influence CTR but are unavailable at scoring time, creating a chicken-and-egg problem between predicted CTR and final ranking. Second,

*Authors contributed equally to this research.

†Work done while at LinkedIn.

online recommendation systems require strict offline-online consistency, yet tracking delays and session-level scoring create gaps between training and serving conditions. Third, production environments demand training stability and reproducibility to ensure reliable business metrics and support rapid experimentation. Fourth, industrial-scale advertising workloads require efficient training and inference systems capable of processing millions to billions of impressions daily.

In this paper, we present CADET (Context-Conditioned Ads Decoder-Only Transformer), an end-to-end decoder-only transformer for ads CTR prediction deployed at LinkedIn. Our approach addresses the above challenges through novel architectural innovations and production engineering techniques.

Our key contributions are as follows:

- **Context-conditioned decoding architecture:** A novel multi-tower decoding block that explicitly models post-scoring contextual signals (e.g., ad position) through K prediction heads, resolving the ranking dependency loop without iterative re-scoring.
- **Self-gated attention mechanism:** An improved self-attention design with representation-level and interaction-level gating that stabilizes training and mitigates pathological attention behaviors, enabling reliable convergence at scale.
- **Temporal encoding with modified RoPE:** A timestamp-based rotary positional encoding that captures time differences ranging from seconds to months, replacing sequence position with event timestamps for ads-specific temporal modeling.
- **Session masking for offline-online consistency:** Customized masking strategies that prevent the model from attending to unavailable in-session events during training, addressing train-serve skew caused by tracking delays.
- **Production engineering at scale:** A comprehensive set of optimizations including tensor packing, sequence chunking, and custom Flash Attention kernels for multi-item scoring that enable efficient training on large-scale datasets and low-latency serving.

The remainder of this paper is organized as follows. Section 2 reviews related work on CTR prediction and sequence-based recommendation. Section 3 details the CADET architecture including the context-conditioned decoding block, self-gated attention, and masking strategies. Section 4 describes productionization techniques for training and serving at scale. Section 5 presents experimental results including ablation studies and online A/B test metrics. Section 6 discusses alternative approaches we considered. Section 7 concludes with a summary.

2 Related Work

We discuss related work from two key areas: (1) ads CTR prediction and post-scoring context handling, and (2) sequence-based recommendation models.

2.1 Ad CTR Prediction and Post-Scoring Context

Ads CTR prediction has been a fundamental task in online advertising. Over the past decade, deep learning models such as

DCN [17, 18], DIN [24] and DHEN [23] have become the dominant approach due to their enhanced capacity for automatic feature interaction learning.

An interesting challenge in CTR prediction as well as other recommendation tasks is handling post-scoring contextual information, such as ad position or UI treatments, which can be unavailable at scoring time but influence user behavior. A simple approach treats position as a debiasing feature—including it during training but omitting it at inference time. More sophisticated methods involve counterfactual learning [1] to explicitly model position bias, or employing secondary factorized models [2] to capture context-dependent effects.

2.2 Sequence-Based Recommendation Models

User activity data in recommendation systems can naturally be represented as sequences. Transformer architectures, which have achieved remarkable success in language and vision domains, have been adapted for recommendation tasks. Many works integrate transformers as sequence encoders within existing DLRM architectures, which have been successfully deployed in industrial systems [3, 20, 21].

More recently, HSTU-style generative recommenders [22] reformulated recommendation as a generative paradigm, where transformers serve as the sole backbone architecture rather than being ensembled with DLRM models. These decoder-only models are trained autoregressively and support both retrieval (directly predicting the next item) and ranking (performing discriminative tasks). Building on this paradigm, models like OneRec [8] perform end-to-end generation to predict the next item without requiring cascaded retrieval-ranking stages.

3 Enhancing Decoder-Only Transformer for Ads System

3.1 Overall Architecture

Inspired by the HSTU ranking architecture [22], the full model processes interleaved ad impression and action sequences:

Input Sequence Formulation: The input to our model consists of a concatenated sequence of static user features followed by interleaved impression and contextualized action tokens:

$$\mathbf{x} = [M; I_1, (C_1, A_1); I_2, (C_2, A_2); \dots; I_{L-1}, (C_{L-1}, A_{L-1}); I_L] \quad (1)$$

where:

- M represents user static features (e.g., profile)
- I_t represents the t -th impression features, a concatenation of:
 - Ad features (e.g., adId)
 - Request features (e.g., device type)
 - Other impression-related features
- C_t represents post-scoring contextual features not available at online scoring time (e.g. ad position)
- A_t represents the action taken on impression t (e.g., click)

Decoder-Only Transformer: A decoder-only transformer processes the interleaved input sequence and predicts all the actions for each impression in one go during training time (i.e. teacher forcing).

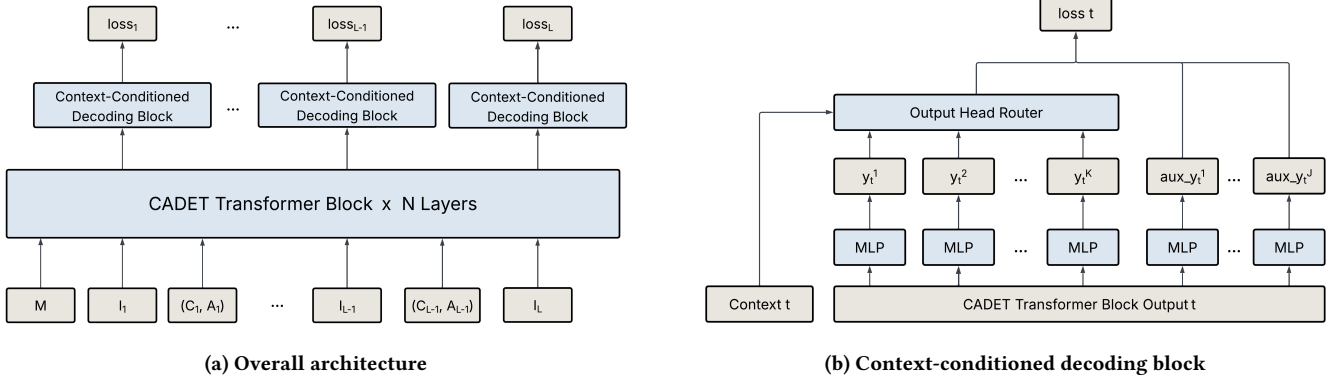


Figure 1: Architecture of the proposed model. (a) Overall architecture showing the interleaved impression-action sequence processing through the decoder-only transformer. (b) Detailed view of the context-conditioned decoding block with multiple prediction heads.

Context-Conditioned Decoding Block: The decoder-only transformer outputs a sequence of predictions paired with contextual metadata for each impression. For each impression, the decoding block produces K context-conditioned predictions:

$$\{\hat{y}_1, \hat{y}_2, \dots, \hat{y}_K\} \quad (2)$$

where \hat{y}_k represents the prediction for context bucket k (e.g., different ad positions). Through this context-conditioned decoding block, described in Section 3.3, the model learns to produce predictions conditioned on post-scoring contextual information.

3.2 CADET Transformer Block

3.2.1 Self-Gated Multi-Head Attention. To improve training stability and mitigate pathological attention behaviors in our proposed model, we introduce self-gated attention [6] that adaptively regulates information flow at both representation and interaction levels; see Figure 2. Unlike output-level gating used in prior work [14, 22], our approach applies gating *before* attention computation on input representations and query-key projections.

Specifically, let $X \in \mathbb{R}^{B \times L \times d_{\text{model}}}$ denote the token representations at each layer of the decoder-only transformer, where B is batch size, L is sequence length and d_{model} is the model dimension. Queries Q and keys K are obtained through linear projections of X and preserve the same dimensionality, i.e., $Q, K \in \mathbb{R}^{B \times L \times d_{\text{model}}}$

$$Q = XW_Q, \quad K = XW_K, \quad (3)$$

where $W_Q, W_K \in \mathbb{R}^{d_{\text{model}} \times d_{\text{model}}}$. We first apply a lightweight self-gating module to obtain gated representations, where the gate is conditioned on the representations themselves. This **representation-level gating** acts as adaptive feature selection, suppressing noisy or low-utility dimensions before attention computation, thereby improving activation scaling and gradient conditioning during training.

$$Gate(X) = \sigma(W_X^{\text{gate}} X), \quad \tilde{X} = X \odot Gate(X) \quad (4)$$

where $\sigma(\cdot)$ is the sigmoid function, \odot denotes element-wise multiplication, and $W_X^{\text{gate}} \in \mathbb{R}^{d_{\text{model}} \times d_{\text{model}}}$.

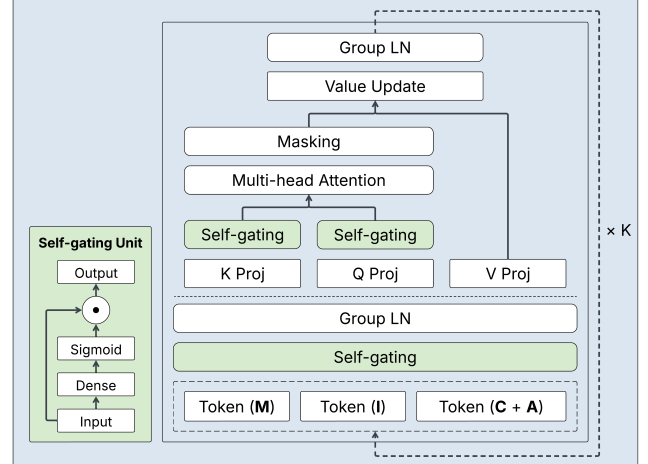


Figure 2: Detailed description of self-gated attention module

In addition, we incorporate self-gating directly into the attention mechanism by modulating the projected queries Q and keys K . This **interaction-level gating** explicitly regulates query-key interactions by constraining dot-product magnitudes, preventing dominant tokens from monopolizing attention and effectively mitigating attention sink phenomena.

$$\begin{aligned} Gate(Q) &= \sigma(W_Q^{\text{gate}} Q), \quad \tilde{Q} = Q \odot Gate(Q) \\ Gate(K) &= \sigma(W_K^{\text{gate}} K), \quad \tilde{K} = K \odot Gate(K) \end{aligned} \quad (5)$$

where $W_Q^{\text{gate}}, W_K^{\text{gate}} \in \mathbb{R}^{d_{\text{model}} \times d_{\text{model}}}$.

3.2.2 Temporal Encoding. We encode temporal information using a modified form of Rotary Positional Embeddings (RoPE) [16]. In the original RoPE formulation, a query or key vector $\mathbf{x} \in \mathbb{R}^d$ is decomposed into $d/2$ two-dimensional components, and the i -th component is rotated by an angle

$$\alpha_i(p) = p \cdot \theta_i, \quad \theta_i = 10000^{-\frac{2i}{d}},$$

where p denotes the item’s sequence position. The dot product between rotated queries and keys will depend on the relative differences in angles, allowing the model to learn about the meaning of relative position differences.

For ads modeling, we care more about differences in time than sequence position, so we replace position p with a Unix timestamp t . To handle time differences ranging from seconds to months, we define the rotation angle for the i -th component as

$$\alpha_i(t) = t \cdot \theta_i, \quad \theta_i = \frac{\phi_{\min}}{\Delta t_{\max}} \cdot \text{base}^{\frac{2i}{d}},$$

where Δt_{\max} is the lookback window used in constructing sequences and thus the largest possible difference in timestamps. ϕ_{\min} is a tunable parameter that lets us control what the the smallest relative rotation (difference in α_0) would be for items with timestamps differing by Δt_{\max} , and base is a tunable parameter that lets us control the highest frequency rotations that are useful for representing short-term information.

We do not add explicit information about sequence position, as causal transformers can learn this implicitly [11].

3.2.3 Customized Masking. We employ customized time-based masking strategies during training and inference to ensure offline-online consistency and efficient candidate scoring.

Inference-time Masking. At scoring time, the ranking model needs to rank hundreds of candidates simultaneously. Similar to previous work on generative recommenders [22], instead of scoring candidates individually, we append all candidates to the end of the sequence and employ a special mask as shown in Figure 3 so that all candidates are scored in a single forward pass while remaining causally isolated from each other. This significantly improves evaluation and online inference speed.

Training Masking. A critical challenge in production recommendation systems is maintaining offline-online consistency. For online ranking systems, recent activity may be unavailable for several reasons, including unavoidable system delay, simultaneous ranking for multiple ad slots, and delayed user interactions (e.g., a user clicking on an ad they saw earlier in the session). Attending to immediately previous tokens in the same session could inflate offline metrics and cause reliance on information unavailable at inference time.

To prevent the model from learning to depend on interactions that are unavailable at inference-time, we enforce session-aware masking during training. We apply a train-time mask M that prevents tokens from attending to same-session information:

$$M_{i,j} = \begin{cases} -\infty & \text{if } t_j > t_i - \Delta_{\text{delay}} \\ 0 & \text{otherwise} \end{cases} \quad (6)$$

where Δ_{delay} encodes the minimum latency we guarantee between an event and its observability online. We materialize this mask at runtime as shown in Figure 3. The final attention computation is:

$$\text{Attention}(Q, K, V) = \text{softmax}\left(\frac{QK^T}{\sqrt{d_k}} + M\right)V \quad (7)$$

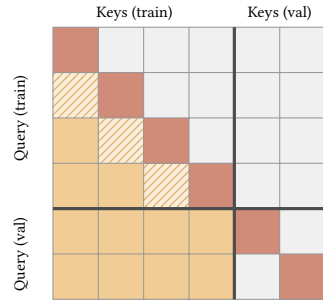


Figure 3: Session-aware masking strategies (depicted before item/action interleaving). Solid yellow cells are always unmasked. Striped cells fall within the Δ_{delay} threshold, masked during training, but available at inference. Gray cells are masked and dark red cells denote the preserved diagonal.

3.3 Context-Conditioned Decoding Block

The decoding block addresses a fundamental challenge in ads recommendation: the gap between training-time observability and inference-time constraints. Critical contextual signals, such as final ad position or specific UI treatments, are often unknown during initial scoring. We resolve this by employing a multi-tower architecture that generates predictions conditioned on potential rendering contexts in a single forward pass.

3.3.1 Context-Conditioned Heads. To model behavior influenced by post-scoring context, we partition the context space into K discrete buckets based on historical click-through rates (e.g., $k = 1$ for position 1, $k = 2$ for positions 2–4, $k = 3$ for positions 5+). For each bucket $k \in \{1, \dots, K\}$, we define a dedicated prediction head branching from the shared transformer output h_t :

$$\hat{y}_k = \text{MLP}_k(h_t) \quad (8)$$

where h_t is the transformer representation for impression t and \hat{y}_k denotes the logit produced by the k -th head.

Training: During training, for each impression t , we observe its ground-truth context bucket $k_t \in \{1, \dots, K\}$. Only the head corresponding to the realized context contributes to the loss:

$$\mathcal{L}_{\text{ctx}} = \sum_{t=1}^L \text{CE}(\hat{y}_{k_t}, y_t) \quad (9)$$

where \hat{y}_{k_t} denotes the prediction from the k_t -th head, and y_t is the ground-truth label. This selective routing ensures each head learns CTR for its specific context while eliminating train-serve mismatch by using position only for loss routing rather than as an input feature.

Serving: At inference time, all K heads produce predictions in parallel, yielding $\{\hat{y}_1, \dots, \hat{y}_K\}$ for each candidate ad. During the online auction, when the serving system renders ads for a specific context, it selects the prediction from the corresponding bucket—e.g., \hat{y}_1 when filling position 1, or \hat{y}_2 when filling positions 2–4. This single-pass approach provides policy-ready signals that resolve the ranking dependency loop without the latency cost of iterative re-ranking or multi-pass feature toggling.

Historical Context Information: As described in Section 3.1, contextual signals C_t are paired with actions A_t rather than included in impression features I_t . This design prevents information leakage during training while enabling the model to learn historical behavior patterns conditioned on context.

3.3.2 Auxiliary Action Heads. To improve representation learning, we introduce auxiliary prediction tasks for fine-grained user actions, including click type classification, landing page dwell time, impression duration regression and other engagement signals. These auxiliary tasks are used solely for training-time regularization and do not participate in serving-time inference. Accordingly, auxiliary heads are implemented as shared prediction modules:

$$\hat{y}_j^{\text{aux}} = \text{MLP}_j(h_t) \quad (10)$$

where j indicates the j -th auxiliary head. Since auxiliary tasks are not required to produce context-conditioned predictions at inference time, we avoid introducing context-specific auxiliary towers. If contextual sensitivity is beneficial for a particular auxiliary signal, contextual features can be incorporated directly into the auxiliary head during training, without affecting the inference-time architecture.

3.3.3 Loss Construction. The total loss combines context-conditioned heads, auxiliary heads, and a pairwise ranking loss:

$$\mathcal{L} = \lambda_{\text{ctx}} \mathcal{L}_{\text{ctx}} + \sum_{j=1}^J \lambda_j \mathcal{L}_j^{\text{aux}} + \lambda_{\text{pair}} \mathcal{L}_{\text{pair}} \quad (11)$$

where J is the number of auxiliary tasks, $\mathcal{L}_j^{\text{aux}}$ denotes the auxiliary loss for task j , $\mathcal{L}_{\text{pair}}$ is the pairwise ranking loss, and $\{\lambda_{\text{ctx}}, \lambda_j, \lambda_{\text{pair}}\}$ are hyperparameters balancing the loss terms.

We adopt the RankNet pairwise loss [4], which has demonstrated empirical performance in large-scale industrial settings [12]. Compared to pointwise objectives, pairwise loss functions directly optimize relative ordering between positive and negative samples, which is better aligned with the ranking nature of ad serving systems where only relative scores determine exposure. Prior work has shown that pairwise approach is particularly suitable under severe class imbalance and noisy labels [4, 5, 13, 19]. The loss is defined as:

$$\mathcal{L}_{\text{pair}} = -\frac{1}{N_+ N_-} \sum_{i=1}^{N_+} \sum_{j=1}^{N_-} \log \left(\sigma \left(z_i^{(+)} - z_j^{(-)} \right) \right) \quad (12)$$

where N_+ and N_- denote the numbers of positive and negative samples within a training batch, respectively. Here, $z_i^{(+)}$ and $z_j^{(-)}$ represent the logits of the i -th positive sample and the j -th negative sample. This formulation constructs a cross-user pairwise loss that explicitly encourages higher scores for positive samples relative to negative ones.

4 Productionization and Scaling

4.1 Training System

We train on NVIDIA H200 GPUs using PyTorch Hybrid Sharded Data Parallel (HSDP) and FlexAttention [9] to support customized masking. We also employ several techniques to improve training efficiency and compress the model size.

4.1.1 Data Processing. The transition to an auto-regressive paradigm allowed us to densify our training data. We migrated from a legacy pointwise architecture where each ad impression was stored as an independent record with over 100 features to a user-centric sequence format. By aggregating impressions and actions into unified sequences and pruning the feature set to high-utility signals, we achieve significant data footprint reduction while maintaining model accuracy by prioritizing temporal behavioral signals (see Section 5.2 for quantitative results).

4.1.2 HSDP. For our model workloads, Hybrid Sharded Data Parallel (HSDP) outperforms pure DDP or FSDP because it reshapes communication to match hardware topology. HSDP shards parameters, gradients, and optimizer state *within* each node, so the frequent collectives (e.g., parameter all-gathers and reduce-scatter of gradients) run over high-bandwidth, low-latency intra-node links (NVLink), where they are comparatively cheap. Across nodes, HSDP typically keeps replicas at the node-group level and performs a smaller set of inter-node synchronizations (DDP-style all-reduce on already-sharded/aggregated buffers), which reduces the volume and frequency of traffic over slower, contention-prone interconnects (InfiniBand/Ethernet). The result is that the most communication-intensive work stays within each node, while cross-node traffic is reduced and spread out, improving step time, scaling efficiency, and stability for large, bandwidth-sensitive models.

4.1.3 Gradient Checkpointing. We use gradient checkpointing to reduce the memory usage by trading a small amount of additional recomputation for a substantial reduction in activation footprint, which enables more aggressive batch-size configurations while maximizing utilization of available HBM for maximum throughput.

4.1.4 Packing. Packing is a technique commonly used in transformer training to reduce memory usage, and is particularly valuable for Transformer-based ads CTR prediction. User interaction sequences in advertising are highly right-skewed: most users have only a handful of impressions within the lookback window while a small minority dominate the tail. A common approach to training sequence models materializes a dense (B, L, d_{model}) tensor, but since attention is the only operation requiring explicit sequence structure, the majority of activation memory and MLP compute is wasted on padding tokens.

To densify our training, we make the packed representation the canonical form throughout training and validation. The dataloader compacts every batch into a contiguous token buffer of shape $(\text{total_tokens}, d_{\text{model}})$ together with prefix-sum offsets and sequence-length metadata. Figure 4 contrasts the padding-heavy layout with the packed variant that keeps per-user tokens contiguous. To maintain a fixed total_tokens per batch is critical for stability and `torch.compile`, each worker aggregates user sequences until the packed length approaches a configured budget, pads the final few tokens to hit the exact target, and emits the batch.

4.1.5 Chunking. While packing eliminates wasted computation on padding tokens, processing long sequences remains costly due to the self-attention mechanism’s $O(n^2)$ complexity—doubling sequence length quadruples attention computation and memory requirements. Sequence chunking addresses this by partitioning long

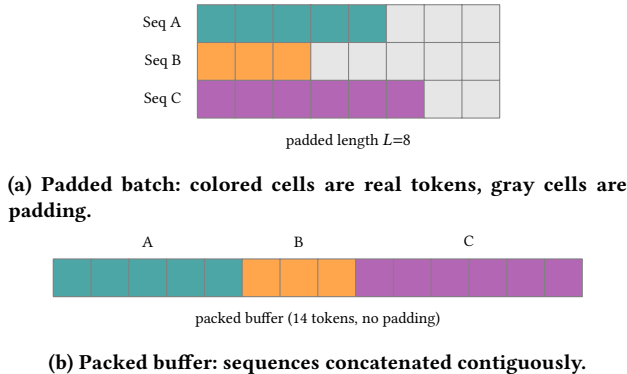


Figure 4: Transition from padded to packed representation. Each color denotes a distinct user sequence; packing eliminates the gray padding and stores only real tokens.

user histories into multiple shorter, non-overlapping chunks, enabling efficient processing of arbitrarily long user histories without the prohibitive cost of full-length attention.

Each chunk becomes an independent training example while preserving temporal ordering. Formally, for a user sequence $S = (s_1, s_2, \dots, s_L)$ ordered from oldest to most recent, we generate $\lceil L/L_{\text{chunk}} \rceil$ training examples by partitioning from the most recent end, where the first chunk contains the most recent tokens. This ensures recent chunks are always full-length. Reducing sequence length from L to L_{chunk} decreases per-sequence attention cost by $(L/L_{\text{chunk}})^2$, with additional savings during offline inference and online serving. This approach is effective because moderate-length sequences already capture the most predictive behavioral signals, exhibiting diminishing returns for extremely long contexts. Furthermore, chunking outperforms naive recent-truncation by retaining older training data that would otherwise be discarded.

4.2 Serving System

The trained model is integrated into an inference service to predict the CTR for ad creatives targeted at LinkedIn users. Each inference request comprises a sequence of the user’s historical interaction context, detailed in Section 3.1, and a list of candidate creatives to be scored. Our primary objective for the inference service is to maximize throughput – defined as the number of requests a GPU can process – while maintaining a p99 latency within a budget of 50ms.

4.2.1 Scaling inference service. Upon receiving a request, each host in the service executes two primary tasks:

- *Preprocessing*: A lightweight CPU task that transforms input features from the historical context and candidate list into the tensor format required for model consumption.
- *Inference*: The execution of the model’s forward() pass on the GPU to generate predictions.

To maintain high GPU utilization, we implement a producer-consumer architecture: a pool of CPU threads executes the feature preprocessing tasks and populates a task queue, which a dedicated GPU thread subsequently drains to perform model inference.

Under this architecture, if the average latency of a single GPU inference is denoted as l ms, the throughput of each host is defined as $1000/l$ requests per second. Consequently, our primary optimization objective is to minimize the latency of individual inference passes by fully leveraging the massive parallel processing capabilities (FLOPS) provided by the GPU.

4.2.2 Custom Flash Attention Kernel. While we use FlexAttention [9] during training to support session masking (Section 3.2), inference requires only the multi-item scoring attention pattern. This simpler, fixed pattern enables us to develop a specialized FlashAttention [7] kernel optimized for inference latency.

Standard PyTorch attention with explicit masks falls back to memory-efficient kernels that lack FlashAttention’s tiled computation and cannot exploit the sparsity of our attention pattern. For context length L and candidate length N , standard kernels execute $(L + N)^2$ operations, whereas our shared-context pattern requires only $L^2/2 + LN$ – linear rather than quadratic in the number of candidates. We developed a custom CUDA kernel extending FlashAttention that exploits this sparsity and integrates with `torch.compile`.

Unlike the standard approach that requires allocating and passing a full 2D attention mask tensor, our kernel accepts only two scalar parameters: `context_length` and `candidate_length`, along with the standard Flash Attention inputs (Q , K , V tensors).

The key insight is that the custom attention pattern is fully determined by these two lengths:

- For query positions $i \leq L$ (context tokens): attend to positions $j \leq i$ (causal mask)
- For query positions $i > L$ (candidate tokens): attend to positions $j \leq L$ (all context) and $j = i$ (self only)

By integrating this masking logic directly into the Flash Attention computation, our kernel achieves several benefits:

- (1) **Eliminated mask materialization**: No need to allocate or transfer a potentially large $O((L + N)^2)$ attention mask tensor to GPU memory.
- (2) **Compute skipping**: During the tiled attention computation, the kernel skips `compute_qk` operations entirely for tiles that are fully masked, rather than computing then masking.
- (3) **Memory efficiency**: Retains Flash Attention’s memory-efficient tiled computation and online softmax.

The kernel implementation modifies the inner loop of Flash Attention to check whether each key-query tile falls within the valid attention region based on the context and candidate length parameters. Tiles that would be entirely masked are skipped without any computation, while boundary tiles apply the appropriate masking logic inline.

5 Experiments and Results

Here we present the results of offline experiments designed to illustrate the contributions of various components of the CADET model, as well as online A/B test results. All experiments are conducted on LinkedIn’s sponsored updates ad click dataset.

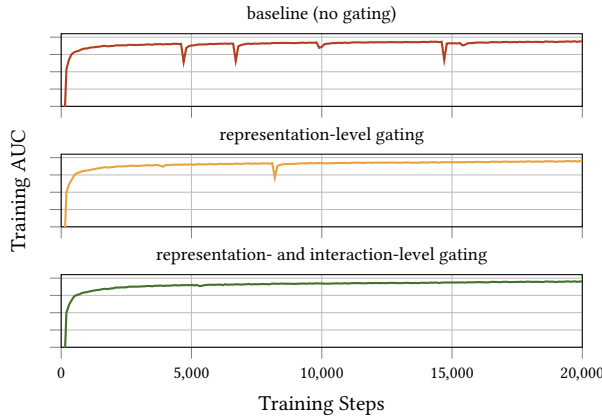


Figure 5: Training AUC curves before 20K steps under different self-gating configurations. Representative samples from multiple runs that exhibited consistent dynamics.

5.1 Ablation Studies on CADET Components

Table 1 shows the results of ablation studies on various model components, measured in relative ROC AUC change compared to the full CADET model. All experiments are performed on one year of data with the final day used for validation and a Δ_{delay} of one hour. We use $n_{\text{layers}} = 8$, $n_{\text{heads}} = 4$, $d_{\text{model}} = 352$, and sequence length $L = 4096$.

5.1.1 Self-Gated Multi-Head Attention. We study the effect of self-gating on training dynamics. Figure 5 shows training AUC over the first 20K steps with the following settings: 1) baseline without gating, 2) representation-level gating, and 3) combined representation- and interaction-level gating. For each setting, we performed multiple runs and consistently observed similar training dynamics. The baseline model exhibits clear instability with multiple sharp AUC drops during training. Representation-level gating substantially smooths the learning trajectory by reducing the frequency and magnitude of these drops. The most stable behavior is achieved when both representation and interaction gating are applied, yielding consistently smooth convergence without pronounced degradations. In practice, the improved stability enhances reproducibility across experiments and production retraining, reduces sensitivity to optimization hyperparameters, and leads to more reliable convergence.

5.1.2 Context-Conditioned Modeling. We use LinkedIn feed position as the context signal in experiments. We set $K = 2$ (positions 1–4, and 5+) to simplify integration with the downstream auction system while capturing the primary position-dependent CTR variation. Removing context-conditioned modeling significantly hurts performance, reducing AUC by 0.61%.

5.1.3 Temporal RoPE. We used $\Delta t_{\text{max}} = 1$ year in milliseconds, $\phi_{\text{min}} = 1e-4$, and $\text{base} = 600000$. Removing RoPE applied to impression timestamps reduces AUC by 0.13%, showing that the model is able to learn the importance of time between impressions.

5.1.4 Session Masking. In this experiment, we retain the Δ_{delay} of one hour when creating attention masks for validation tokens, but set Δ_{delay} to zero otherwise, meaning that during training we allow tokens to attend to any previous token. The drop of 0.31% in AUC shows that the model is indeed harmed by allowing it access to information at training time that would not be available during inference due to latency in updating sequences.

5.1.5 Pairwise Ranking Loss. Removing the pairwise ranking loss term $\lambda_{\text{pair}} \mathcal{L}_{\text{pair}}$ results in a consistent AUC decrease of 0.03%. While the relative offline lift is small, pairwise supervision can help combat exposure bias inherent in logged click data and is low-cost to implement without external data system dependencies. We therefore retain it in our final model.

Model Variant	ΔAUC in validation
full CADET	-
- context conditioned	-0.61%
- temporal RoPE	-0.13%
- session masking	-0.31%
- pairwise loss	-0.03%

Table 1: Ablation Studies

5.2 Scaling and Efficiency

We evaluate the efficiency gains from our productionization techniques described in Section 4.

5.2.1 Data Processing. Transitioning from a pointwise architecture with over 100 features per impression to a user-centric sequence format with 12 high-utility signals reduced our data footprint by 98%. Despite the leaner feature set, the sequence-native design achieves higher accuracy by prioritizing temporal behavioral signals.

5.2.2 Packing. By eliminating padding tokens through packing, we achieve approximately 4 \times increase in effective batch size. This is particularly impactful given the right-skewed distribution of user sequence lengths in advertising, where most users have only a handful of impressions.

5.2.3 Chunking. Table 2 shows the accuracy-efficiency trade-off for sequence chunking. Reducing sequence length from 4096 to 2048 tokens decreases training cost by 54% while incurring only 0.04% AUC degradation, demonstrating that chunking can be an effective way to reduce computation without significantly hurting relevance performance.

Sequence Length	Training Cost	ΔAUC
4096 (baseline)	1.0 \times	—
2048	0.46 \times	-0.04%
1024	0.29 \times	-0.29%

Table 2: Accuracy-efficiency trade-off for sequence chunking.

5.2.4 Inference Optimization. We evaluate our custom Flash Attention kernel on inference requests with 4,096 context tokens and 512 candidate tokens. The baseline fused multi-head attention (fmha) kernel achieves only 34 TFLOPS/s—significantly below the A100’s theoretical peak of 312 TFLOPS/s for FP16 operations. Our custom kernel reduces attention execution time from $792\mu\text{s}$ to $262\mu\text{s}$ —a $3\times$ speedup. This kernel-level efficiency translates to 330 requests per second per GPU while maintaining p99 latency under 50ms.

5.3 Online Results

We evaluated CADET through large-scale online A/B testing on LinkedIn’s homefeed sponsored updates and saw strong online results, with significant improvements to our core business metrics of CTR and Revenue, as shown in Table 3.

Experimental Setup: The control model was the production **LiRank** [3] architecture, a hybrid ensemble utilizing **DCNv2** [18] for feature interactions and **TransAct** [20] for sequential history modeling. For the treatment group, we replaced this entire production ensemble with the unified **CADET** model.

Results: As shown in Table 3, CADET achieved a statistically significant **+11.04%** lift in CTR over the LiRank production baseline. This result is particularly notable because it demonstrates that a unified generative approach can outperform a highly optimized, multi-component hybrid system while simplifying the engineering stack. CADET is able to learn implicit temporal patterns to achieve better relevance results for users with relatively few features.

Metric	Relative Change
CTR	+11.04%
Revenue	+0.14%

Table 3: Online Metrics compared to LiRank baseline

6 Alternative Approaches Considered

During the development of CADET, we explored several alternative architectural choices that ultimately did not make it into the final system. We document these here to provide insight into our design decisions.

HSTU Architecture. We experimented with the HSTU architecture [22], including pointwise aggregation self-attention, removing FFN layers, and relative attention bias. These modifications yielded neutral to marginal gains on our dataset. Given that standard transformer components provide access to well-optimized kernels and libraries such as FlexAttention, we chose to retain the conventional Transformer architecture. This tradeoff may differ across datasets and deployment environments.

Semantic ID Tokenization. We explored using RQ-VAE-based semantic ID tokenization [15] as an alternative to ID-based item representations. Our experiments showed that semantic IDs cannot replace ID-based representations in our setting, likely due to the nature of our ads inventory size. Adding semantic IDs alongside ID-based representations provided marginal improvement (0.02% AUC lift) at the cost of significantly complicating the production

pipeline. Given this trade-off, we opted not to include semantic ID tokenization in our final system.

7 Conclusion

We presented CADET, an end-to-end decoder-only transformer for large-scale ads CTR prediction at LinkedIn. This work addressed key challenges in applying autoregressive transformers to advertising: self-gated attention stabilizes optimization, timestamp-based RoPE captures temporal relationships across timescales, session-aware masking ensures offline-online consistency, and context-conditioned decoding resolves the chicken-and-egg problem between CTR prediction and post-scoring signals.

Beyond modeling innovations, productionization techniques including sequence packing, chunking, and custom FlashAttention kernels enable efficient training and low-latency serving. Empirically, CADET achieves 11.04% CTR lift over our LiRank baseline [3], showing that a unified decoder-only transformer, combined with targeted modeling and production optimizations, can effectively outperform DLRM-style ensemble models in industrial ads ranking.

Acknowledgments

We thank Oren Sar Shalom, Yuan Gao and Franklin Graves for their valuable discussions and paper reviews. We also thank Guandong Zhu, Rutvij Mehta, Serhat Leloglu, Zeyu Jin, Shuzhe Xiao, Oz Ozkan, Hina Arora, Shao Tang, Alex Berlinger, Ankur Agrawal, Emily Ki, Hongzhou Li, Joe Cho, Qian Li, Siva Popuri, Tiffany Zhou, Chen Zhu, Haoyue Tang, Jaideep Ray, Yang Pei, Yujie Ai, Sumit Rangwala, and Xiaoling Zhai for their collaboration and contributions to this work. Finally, we thank Sen Zhou, Xianxing Zhang, Julie Choi, Manas Apte, Yitong Zhou, and Sriram Sankar for their guidance and leadership support.

References

- [1] Aman Agarwal, Kenta Takatsu, Ivan Zaitsev, and Thorsten Joachims. 2019. A General Framework for Counterfactual Learning-to-Rank. In *Proceedings of the 42nd International ACM SIGIR Conference on Research and Development in Information Retrieval*. 5–14. <https://doi.org/10.1145/3331184.3331202>
- [2] Rohan Anil, Sandra Gadano, Da Huang, Nijith Jacob, Zhuoshu Li, Dong Lin, Todd Phillips, Cristina Pop, Kevin Regan, Gil I. Shamir, Rakesh Shivanna, and Qiqi Yan. 2022. On the Factory Floor: ML Engineering for Industrial-Scale Ads Recommendation Models. In *ORSUM@RecSys 2022*. <https://ceur-ws.org/Vol-3303/paper6.pdf>
- [3] Fedor Borisuk, Mingzhou Zhou, Qingquan Song, Siyu Zhu, Birjodh Tiwana, Ganesh Parameswaran, Siddharth Dangi, Lars Hertel, Qiang Charles Xiao, Xiaochen Hou, Yunbo Ouyang, Aman Gupta, Sheallika Singh, Dan Liu, Hailing Cheng, Lei Le, Jonathan Hung, Sathiya Keerthi, Ruoyan Wang, Fengyu Zhang, Mohit Kothari, Chen Zhu, Daqi Sun, Yun Dai, Xun Luan, Siron Zhu, Zhiwei Wang, Neil Daffary, Qianqi Shen, Chengming Jiang, Haichao Wei, Maneesh Varshney, Amol Ghosh, and Souvik Ghosh. 2024. LiRank: Industrial Large Scale Ranking Models at LinkedIn. In *Proceedings of the 30th ACM SIGKDD Conference on Knowledge Discovery and Data Mining (KDD ’24)*. 4804–4815. <https://doi.org/10.1145/3637528.3671561>
- [4] Chris Burges, Tal Shaked, Erin Renshaw, Ari Lazier, Matt Deeds, Nicole Hamilton, and Greg Hullender. 2005. Learning to rank using gradient descent. In *Proceedings of the 22nd international conference on Machine learning*. 89–96.
- [5] Zhe Cao, Tao Qin, Tie-Yan Liu, Ming-Feng Tsai, and Hang Li. 2007. Learning to rank: from pairwise approach to listwise approach. In *Proceedings of the 24th international conference on Machine learning*. 129–136.
- [6] Yekun Chai, Shuo Jin, and Xinwen Hou. 2020. Highway Transformer: Self-Gating Enhanced Self-Attentive Networks. In *Proceedings of the 58th Annual Meeting of the Association for Computational Linguistics*, Dan Jurafsky, Joyce Chai, Natalie Schluter, and Joel Tetreault (Eds.). Association for Computational Linguistics, Online, 6887–6900. <https://doi.org/10.18653/v1/2020.acl-main.616>
- [7] Tri Dao. 2024. FlashAttention-3: Fast and Accurate Attention with Asynchrony and Low-precision. *arXiv preprint arXiv:2407.08608* (2024).

[8] Jiaxin Deng, Shiyao Wang, Kuo Cai, Lejian Ren, Qigen Hu, Weifeng Ding, Qiang Luo, and Guorui Zhou. 2025. OneRec: Unifying Retrieve and Rank with Generative Recommender and Iterative Preference Alignment. arXiv:2502.18965 [cs.IR] <https://arxiv.org/abs/2502.18965>

[9] Juechu Dong, Boyuan Feng, Driss Guessouss, Yanbo Liang, and Horace He. 2024. Flex Attention: A Programming Model for Generating Optimized Attention Kernels. arXiv:2412.05496 [cs.LG] <https://arxiv.org/abs/2412.05496>

[10] Ruidong Han, Bin Yin, Shangyu Chen, Fei Jiang, Xiang Li, Chi Ma, Mincong Huang, Xiaoguang Li, Chunzhen Jing, Yueming Han, MengLei Zhou, Lei Yu, Chuan Liu, and Wei Lin. 2025. MTGR: Industrial-Scale Generative Recommendation Framework in Meituan. In *Proceedings of the 34th ACM International Conference on Information and Knowledge Management (CIKM '25)*. 5731–5738. <https://doi.org/10.1145/3746252.3761565>

[11] Amirhossein Kazemnejad, Inkit Padhi, Karthikeyan Natesan Ramamurthy, Payel Das, and Siva Reddy. 2023. The Impact of Positional Encoding on Length Generalization in Transformers. In *Proceedings of the 37th International Conference on Neural Information Processing Systems (NIPS '23)*. Article 1082.

[12] Zhitian Lin, Junwei Pan, Shangyu Zhang, Ximei Wang, Xi Xiao, Shudong Huang, Lei Xiao, and Jie Jiang. 2024. Understanding the ranking loss for recommendation with sparse user feedback. In *Proceedings of the 30th ACM SIGKDD Conference on Knowledge Discovery and Data Mining*. 5409–5418.

[13] Tie-Yan Liu et al. 2009. Learning to rank for information retrieval. *Foundations and Trends® in Information Retrieval* 3, 3 (2009), 225–331.

[14] Zihan Qiu, Zekun Wang, Bo Zheng, Zeyu Huang, Kaiyue Wen, Songlin Yang, Rui Men, Le Yu, Fei Huang, Suozhi Huang, Dayiheng Liu, Jingren Zhou, and Junyang Lin. 2025. Gated Attention for Large Language Models: Non-linearity, Sparsity, and Attention-Sink-Free. In *Proceedings of the 39th Annual Conference on Neural Information Processing Systems (NeurIPS '25)*.

[15] Shashank Rajput, Nikhil Mehta, Anima Singh, Raghunandan Keshavan, Trung Vu, Lukasz Heidt, Lichan Hong, Yi Tay, Vinh Q. Tran, Jonah Samost, Maciej Kula, Ed H. Chi, and Maheswaran Sathiamoorthy. 2023. Recommender Systems with Generative Retrieval. In *Proceedings of the 37th International Conference on Neural Information Processing Systems (NIPS '23)*. Article 452.

[16] Jianlin Su, Murtadha Ahmed, Yu Lu, Shengfeng Pan, Wen Bo, and Yunfeng Liu. 2024. RoFormer: Enhanced Transformer with Rotary Position Embedding. *Neurocomputing* 568 (2024), 127063. <https://doi.org/10.1016/j.neucom.2023.127063>

[17] Ruoxi Wang, Bin Fu, Gang Fu, and Mingliang Wang. 2017. Deep & Cross Network for Ad Click Predictions. In *Proceedings of the ADKDD'17 (ADKDD'17)*. Article 12, 7 pages. <https://doi.org/10.1145/3124749.3124754>

[18] Ruoxi Wang, Rakesh Shivanna, Derek Cheng, Sagar Jain, Dong Lin, Lichan Hong, and Ed Chi. 2021. DCN V2: Improved Deep & Cross Network and Practical Lessons for Web-scale Learning to Rank Systems. In *Proceedings of the Web Conference 2021 (WWW '21)*. 1785–1797. <https://doi.org/10.1145/3442381.3450078>

[19] Qiang Wu, Christopher JC Burges, Krysta M Svore, and Jianfeng Gao. 2010. Adapting boosting for information retrieval measures. *Information Retrieval* 13, 3 (2010), 254–270.

[20] Xue Xia, Pong Eksombatchai, Nikil Pancha, Dhruvil Deven Badani, Po-Wei Wang, Neng Gu, Saurabh Vishwas Joshi, Nazanin Farahpour, Zhiyuan Zhang, and Andrew Zhai. 2023. TransAct: Transformer-based Realtime User Action Model for Recommendation at Pinterest. In *Proceedings of the 29th ACM SIGKDD Conference on Knowledge Discovery and Data Mining (KDD '23)*. 5249–5259. <https://doi.org/10.1145/3580305.3599918>

[21] Zhichen Zeng, Xiaolong Liu, Mengyue Hang, Xiaoyi Liu, Qinghai Zhou, Chaofei Yang, Yiqun Liu, Yichen Ruan, Laming Chen, Yuxin Chen, Yujia Hao, Jiaqi Xu, Jadi Nie, Xi Liu, Buyun Zhang, Wei Wen, Siyang Yuan, Hang Yin, Xin Zhang, Kai Wang, Wen-Yen Chen, Yiping Han, Huayu Li, Chunzhi Yang, Bo Long, Philip S. Yu, Hanghang Tong, and Jian Yang. 2025. InterFormer: Effective Heterogeneous Interaction Learning for Click-Through Rate Prediction. In *Proceedings of the 34th ACM International Conference on Information and Knowledge Management (CIKM '25)*. 6225–6233. <https://doi.org/10.1145/3746252.3761527>

[22] Jiaqi Zhai, Lucy Liao, Xing Liu, Yueming Wang, Rui Li, Xuan Cao, Leon Gao, Zhaojie Gong, Fangda Gu, Jiayuan He, Yinghai Lu, and Yu Shi. 2024. Actions Speak Louder than Words: Trillion-Parameter Sequential Transducers for Generative Recommendations. In *Proceedings of the 41st International Conference on Machine Learning (ICML '24)*. PMLR, 58484–58509. <https://proceedings.mlr.press/v235/zhai24a.html>

[23] Buyun Zhang, Liang Luo, Xi Liu, Jay Li, Zeliang Chen, Weilin Zhang, Xiaohan Wei, Yuchen Hao, Michael Tsang, Wenjun Wang, Yang Liu, Huayu Li, Yasmine Badr, Jongsoo Park, Jiyun Yang, Dheevatsa Mudigere, and Ellie Wen. 2022. DHEN: A Deep and Hierarchical Ensemble Network for Large-Scale Click-Through Rate Prediction. arXiv:2203.11014 [cs.IR] <https://arxiv.org/abs/2203.11014>

[24] Guorui Zhou, Xiaoqiang Zhu, Chenru Song, Ying Fan, Han Zhu, Xiao Ma, Yanghui Yan, Junqi Jin, Han Li, and Kun Gai. 2018. Deep Interest Network for Click-Through Rate Prediction. In *Proceedings of the 24th ACM SIGKDD International Conference on Knowledge Discovery & Data Mining (KDD '18)*. 1059–1068. <https://doi.org/10.1145/3219819.3219823>